Mon. Not. R. Astron. Soc. **399,** 1576–1586 (2009) doi:10.1111/j.1365-2966.2009.15378.x

Swift observations of GW Lib: a unique insight into a rare outburst

K. Byckling,[1⋆] J. P. Osborne,[1] P. J. Wheatley,[2] G. A. Wynn,[1] A. Beardmore,[1] V. Braito,[1] K. Mukai[3] and R. G. West[1]

[1]*Department of Physics and Astronomy, University of Leicester, University Road, Leicester LE1 7RH*
[2]*Department of Physics, University of Warwick, Coventry CV4 7AL*
[3]*NASA/Goddard Space Flight Center, Greenbelt, MD 20771, USA*

Accepted 2009 July 10. Received 2009 July 1; in original form 2009 March 26

ABSTRACT

The second known outburst of the WZ Sge type dwarf nova GW Lib was observed in 2007 April. We have obtained unique multiwavelength data of this outburst which lasted ∼26 days. The *American Association of Variable Star Observers* (*AAVSO*) recorded the outburst in the optical, which was also monitored by *Wide Angle Search for Planets*, with a peak *V* magnitude of ∼8. The outburst was followed in the ultraviolet and X-ray wavelengths by the *Swift* ultraviolet/optical and X-ray telescopes. The X-ray flux at optical maximum was found to be three orders of magnitude above the pre-outburst quiescent level, whereas X-rays are normally suppressed during dwarf nova outbursts. A distinct supersoft X-ray component was also detected at optical maximum, which probably arises from an optically thick boundary layer. Follow-up *Swift* observations taken 1 and 2 years after the outburst show that the post-outburst quiescent X-ray flux remains an order of magnitude higher than the pre-outburst flux. The long interoutburst time-scale of GW Lib with no observed normal outbursts support the idea that the inner disc in GW Lib is evacuated or the disc viscosity is very low.

Key words: accretion, accretion discs – stars: dwarf novae – novae, cataclysmic variables – X-rays: binaries – X-rays: stars.

1 INTRODUCTION

Dwarf novae (DNe) are non-magnetic cataclysmic variables (CVs) with accretion discs and a white dwarf primary and a main-sequence secondary star. They are relatively nearby sources which provide a laboratory for studying accretion disc physics in our Galaxy. The orbital periods of DNe are typically between 70 min and 10 h. From time to time, the disc goes into an outburst which is a brightening of the disc by 2–9 mag and which can last from days to several weeks. The mechanism leading to a DN outburst is thought to be a disc instability which was first proposed by Hoshi (1979) [for a more detailed discussion, see Lasota (2001)]. After this luminous phenomenon, the system returns to quiescence which can last from ∼10 days to decades. The disc dominates the optical emission during an outburst. SU UMa type DNe show superoutbursts which can last for several weeks and are characterized by superhumps, periodic brightenings whose recurrence times are slightly longer than the orbital period. Superhumps are thought to be due to a 3:1 resonance in the accretion disc (Whitehurst 1988). While most SU UMa types show normal outbursts and superoutbursts, a subset called the WZ Sge stars only have superoutbursts. A typical feature of superoutbursts is a plateau phase in the optical light curve lasting for several days.

GW Lib was discovered in 1983 when it went into an outburst (Maza & Gonzalez 1983). It was present in the European Southern Observatory B Survey plates at magnitude 18.5 preceding the 1983 outburst. GW Lib brightened by 9 mag during the outburst and later faded back to the quiescent state, and thus was classified as a nova. Later studies showed that the spectrum resembled a DN in quiescence (Duerbeck & Seitter 1987). Since 1983, no other outbursts of GW Lib had been observed until that of 2007 April 12 (Templeton 2007). This outburst, which was recorded by the *AAVSO* observers, *Wide Angle Search for Planets (WASP)-South* and by *Swift*, lasted for 26 days. The brightest optical magnitude was reached at ∼8 mag in the *V* band. GW Lib has been classified as a WZ Sge type star due to its short period ($P_{\rm orb} = 76.78$ min; Thorstensen et al. 2002) and low accretion rate (van Zyl et al. 2004). Typical characteristics of WZ Sge type stars are short orbital periods, low mass-transfer rates and extremely long recurrence times which can last for decades. GW Lib was the first observed CV in which the accreting white dwarf showed non-radial pulsations (Warner & van Zyl 1998). This phenomenon was not expected to be discovered in accreting binaries since they were considered to be too hot to contain non-radially pulsating white dwarfs, although low mass-transfer rates from the secondary would explain low net accretion rates on to the white dwarf, and thus a lower accretion heating of the white dwarf (van

⋆E-mail: kjkb2@star.le.ac.uk

Zyl et al. 2000). The pulsations of white dwarfs are thought to be due to g-mode non-radial gravity waves (Koester & Chanmugam 1990). In GW Lib, pulsations are seen near 230, 370 and 650 s in the optical waveband (e.g. *SAAO* data), and also in the *Hubble Space Telescope* (*HST*) ultraviolet (UV) data but with approximately six times higher amplitudes than in the optical (Szkody et al. 2002). An *XMM–Newton* observation of GW Lib obtained in 2005 during its quiescent state reveals that these pulsations are also present in the *XMM–Newton* Optical Monitor (OM) data, but not seen in the X-ray data (Hilton et al. 2007). These *XMM–Newton* observations also confirmed that GW Lib has a very low accretion rate during quiescence.

In this paper, we present the 2007 outburst light curves of GW Lib in the optical (*AAVSO* and *WASP-South*), UV [*Swift*, UV/optical telescope (UVOT)] and X-ray [*Swift*, X-ray telescope (XRT)] bands. We also present X-ray spectral analysis of the outburst observations and follow-up *Swift* observations of GW Lib in 2008 and 2009. Previous multiwavelength observations covering outbursts of SU UMa (and WZ Sge) type systems have been obtained from, for example, VW Hyi (Pringle et al. 1987; Wheatley et al. 1996b), WZ Sge (Kuulkers et al. 2002; Wheatley & Mauche 2005) and OY Car (Mauche & Raymond 2000). Multiwavelength observations of DNe are needed in order to enhance our knowledge of astrophysical systems with discs, e.g. X-ray binaries and active galactic nuclei. DN outbursts offer a good opportunity to study the disc physics, and compare the current theory of outbursts with the observational information. The fact that GW Lib does not show any normal outbursts and the recurrence time between the two major outbursts was over 20 years suggests that the disc structure could be different from most other DNe.

2 OBSERVATIONS AND DATA REDUCTION

GW Lib was initially observed by the *Swift Gamma-ray Burst Explorer* (Gehrels et al. 2004) between 2007 April 13 and May 16, over an interval of 30 days. The data were obtained with the UVOT (Roming et al. 2005) and the XRT (Burrows et al. 2005) which has an energy resolution of 140 eV at 5.9 keV (at launch) (see Capalbi et al. (2005), $R \sim 40$). The XRT was operating in the Window Timing (WT) and Photon-Counting (PC) modes during the observations. The UVOT observations were obtained in the imaging mode with the UV grism in order to provide spectral information and to mitigate against coincidence losses. The resolution of the UV grism is $R \sim 150$ for 11–15 mag range stars[1] The details of the 38 observations are listed in Table 1. The first two observations were obtained in imaging mode with the *UVM2* filter, but these suffer from severe coincidence loss effects and were thus excluded from our analysis. The optical data were provided by the *AAVSO* observers and by the *Wide Angle Search for Planets* (Pollacco et al. 2006).

In addition to the outburst observations, follow-up *Swift* observations of GW Lib were made in 2008 April–May and 2009 February–March. For these observations, the *V* and *UVW1* filters were used in the UVOT instrument. The details of these observations are also given in Table 1.

2.1 UV grism data reduction

The *Swift* UV grism was operating in clocked mode at the time of the outburst observations. We have used our own automated pipeline, based around UVOT *Swift* FTOOLS (Immler et al. 2006) for the spectral extraction of the UV grism data. The release version which we used (HEASOFT v.6.1.2) of the *Swift* UVOT analysis software does not allow grism spectra to be traced, nor extracted optimally. Thus, under FTOOLS, we were restricted to using a box extraction of a fixed width for both source and background regions. The extraction box must be well centred, aligned in so far as is possible with the dispersion direction and broad enough that slight miscentrings do not preferentially exclude flux from the wings of the extracted spectra at specific wavelengths. For a well-centred box, a width of 35 pixels contains 90 per cent of the integrated source counts, and this was the width chosen. Larger slit widths increase the source counts at the expense of increased background noise. Thus, larger slit widths do not enhance the statistical quality, and further increase the likelihood of contamination by nearby sources. For the background, we used extraction widths of 25 pixels.

After having chosen our source and background regions for each observation, the images were corrected for modulo-8 fixed pattern noise, and source and background spectra were extracted automatically using the FTOOL UVOTIMGRISM. Response functions were then created with UVOTRMFGEN. Unfortunately, the last 39 spectra from 2007 May 10 onwards were taken at a roll angle which placed a nearby source (TYC6766-1570-1) on a line between our source and in the same direction as the dispersion direction. These spectra were severely contaminated and we therefore exclude them from our analysis. The wavelength range of the UV data for the light curve was restricted to 2200–4000 Å due to contamination by other zeroth-order spectra in the short-wavelength end.

The 2008 and 2009 observations were obtained in filter mode. We derived the *V* and *UVW1* ($\bar{\lambda} = 2600$ Å) fluxes and magnitudes using the FTOOL UVOTMAGHIST. The source counts were extracted by using circular extraction region with $r_{\rm src} = 5$ arcsec. A circular background region with a radius of $r_{\rm bg} = 10$ arcsec was placed on a source-free region in the field of view.

2.2 X-ray data reduction

The X-ray data reduction was performed with the standard *Swift* pipelines retaining grades 0–12 for the PC mode and 0–2 for the WT mode data. The *Swift* X-ray data cover the energy range 0.3–10 keV, but the source is detected only up to 8.0 keV. The X-ray light curve was extracted from the WT and PC mode data by using the tools described in Evans et al. (2009).

The X-ray spectra were extracted with XSELECT. For the WT mode data, a 40 pixel (94 arcsec) box for the source and an 80 pixel (189 arcsec) box for the background region were used. The normal limit for pile-up in WT mode data is $\sim$100 ct s^{-1} (Romano et al. 2006), thus it was not necessary to account for this when extracting the spectra. The PC mode source data were extracted using a 20 pixel (47 arcsec) circle and the background data within a 60 pixel (141 arcsec) circular area. The PC mode data from the first observation were not used for spectral extraction. The point spread functions of the rest of the PC mode data were checked to verify that pile-up did not occur.

2.3 WASP data reduction

GW Lib falls into a field which was being intensively monitored by the *WASP* search for transiting exoplanets (Pollacco et al. 2006) at the time of the outburst. The *WASP* is a wide-field imaging system with each instrument having a field of view of 482 deg^2. The photometric accuracy of the instruments is better than

[1] http://heasarc.gsfc.nasa.gov/docs/swift/analysis/uvot_ugrism.html

Table 1. The *Swift* observations of GW Lib obtained in 2007, 2008 and 2009.

ObsID	$T_{\rm start}$	Roll angle (°)	UVOT exposure (s)	XRT WT exposure (s)	XRT PC exposure (s)	Ugrism exposure (s)
30917001	2007-04-13T15:19:47	133	4914	2902	1910	0
30917002	2007-04-18T06:22:00	136	4781	4755	0	0
30917003	2007-04-20T17:53:57	141	992	5	990	992
30917004	2007-04-21T03:47:02	142	769	4	772	769
30917005	2007-04-21T14:55:01	142	904	2	910	904
30917006	2007-04-21T22:56:00	142	1442	4	1447	1442
30917008	2007-04-22T23:02:00	142	1264	2	1271	1264
30917009	2007-04-23T11:42:01	142	1050	8	1048	1050
30917010	2007-04-24T00:50:00	142	1352	13	1349	1352
30917011	2007-04-24T13:38:01	142	1288	4	1294	1288
30917012	2007-04-25T02:38:00	142	1635	6	1639	1635
30917013	2007-04-25T12:15:01	142	1632	10	1634	1632
30917014	2007-04-26T02:50:01	142	1393	5	1400	1393
30917015	2007-04-26T20:30:01	142	1344	6	1350	1344
30917016	2007-04-27T02:28:00	155	5868	12	5890	5868
30917017	2007-04-29T01:05:00	155	5643	15	5659	5643
30917018	2007-05-01T01:18:01	168	3150	6	3162	3150
30917019	2007-05-05T09:46:01	168	1597	3	1605	1597
30917020	2007-05-05T22:38:01	168	1596	2	1605	1596
30917022	2007-05-07T00:20:00	151	1589	9	1588	1589
30917023	2007-05-07T11:35:01	151	1358	2	1364	1358
30917024	2007-05-07T22:50:00	151	1595	7	1590	1595
30917025	2007-05-08T10:09:00	156	1294	2	1294	1294
30917026	2007-05-08T21:24:01	156	1247	2	1249	1247
30917027	2007-05-09T08:41:00	156	875	6	872	875
30917028	2007-05-09T19:49:01	156	1496	2	1504	1496
30917029	2007-05-10T00:45:01	162	1457	4	1462	1457
30917030	2007-05-10T18:19:00	162	1577	4	1582	1577
30917031	2007-05-11T07:10:01	162	1433	3	1439	1433
30917032	2007-05-11T18:25:01	162	1369	5	1371	1369
30917033	2007-05-12T07:16:00	162	1372	10	1366	1372
30917034	2007-05-12T18:31:00	162	1372	2	1379	1372
30917035	2007-05-13T05:46:01	162	1157	4	1161	1157
30917036	2007-05-13T18:37:00	162	1313	4	1319	1313
30917037	2007-05-14T07:28:01	162	1373	4	1377	1373
30917038	2007-05-14T18:42:01	162	1250	3	1255	1250
30917039	2007-05-15T07:34:01	162	1400	2	1406	1400
30917041	2007-05-16T04:27:01	162	1947	6	1956	1947
30917042	2008-04-24T17:33:01	150	4772	0	4959	0
30917043	2008-05-01T18:25:09	173	83	0	122	0
30917044	2008-05-08T12:38:01	151	1612	0	1627	0
30917045	2009-02-22T02:16:00	111	5939	0	5779	0
30917046	2009-03-02T03:10:01	112	4536	0	4586	0

1 per cent for objects with V magnitude ∼7.0–11.5. The field (centred on 15 h 02 m, −28 d 22 m) was observed between 2007 February 16 and 2007 July 19, with an average of 88 images per night, each with an exposure time of 30 s. The data were extracted and calibrated in automated fashion using the standard *WASP* pipeline, full details of which are given in Pollacco et al. (2006).

3 TIME SERIES ANALYSIS

3.1 Outburst light curves

Fig. 1 presents the 2007 April–May outburst of GW Lib. The top panel shows the *AAVSO* V-band light curve in black and the *WASP* light curve (V+R bands) in light grey (light blue in the online version) (scaled to match the *AAVSO* V-band magnitude). The magnitudes have been converted to log F in order to make comparison between the optical and UV light curves clearer. The middle and lower panels show the UV and X-ray light curves, respectively. The *AAVSO* outburst light curve is already rising from magnitude 13 ($\log F \approx -13.6$ erg cm^{-2} s^{-1} Å^{-1}) on JD 245 4203.1 which we define as T_0. It reaches its highest peak one day later at magnitude 7.9 ($\log F \approx -11.7$ erg cm^{-2} s^{-1} Å^{-1}), and after the peak declines steadily for 23 days. At 29 days after the beginning of the outburst, the optical brightness declines sharply to magnitude ∼14 ($\log F \approx -14.2$ erg cm^{-2} s^{-1} Å^{-1}), presumably as the accretion disc returns to its quiescent state. Large variations in the *WASP* light curve around day $T_0 + 11$, resulting from poor weather conditions, were excluded.

The rise of the UV emission for GW Lib was not observed, and so we are not able to quantify any UV delay, such as that previously measured by, for example, Hassall et al. (1983) in VW Hyi. However, the system is already extremely UV bright at the

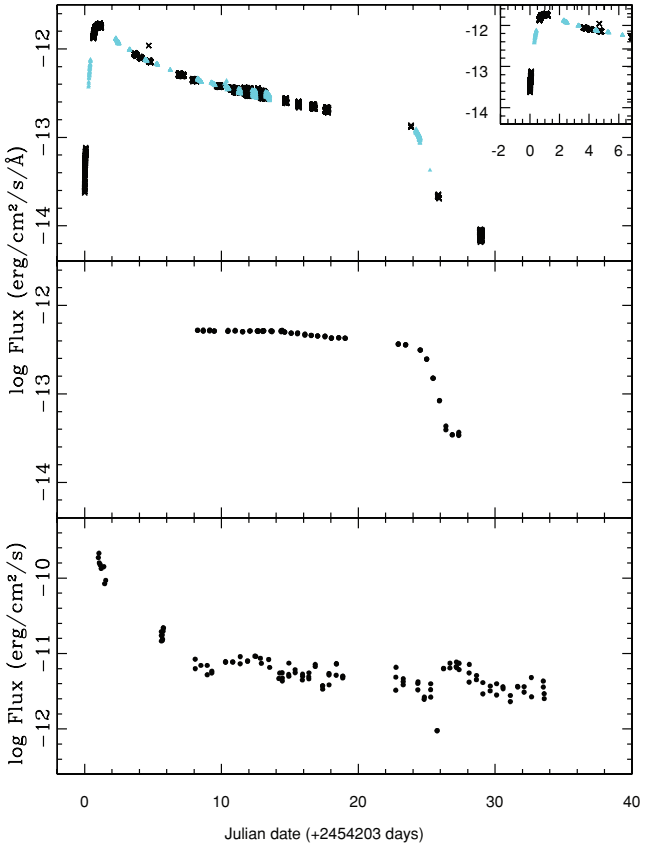

Figure 1. The optical, UV and X-ray outburst light curves of GW Lib. T_0 is JD 245 4203.1, which corresponds to the start time of the first data point in the *AAVSO* light curve. The top panel shows the *AAVSO* optical light curve (www.aavso.org) in the *V* band (converted to log *F*) in black and the *WASP* light curve in light grey (see the text for details). The upper panel inset shows the rapid rise to maximum peaking one day after the onset of the outburst. The middle panel shows the UV in the wavelength range 2200–4000 Å (*Swift* UV grism) and the bottom panel the X-ray light curve in 0.3–10.0 keV (*Swift* XRT). The X-ray data have been binned at 600 s and the other bands are plotted per exposure.

time of the first *Swift* observations, 1 day after the beginning of the outburst, when the *UVM2* filter was used. Unfortunately, these two observations are far too overexposed to provide useful flux measurements and they are not shown in our light curve. Our UV light curve (from the UVOT grism data) starts 8 days after the onset of the outburst. It remains almost flat for ∼6 days and then starts to decline. At 24.5 days after the optical rise, the UV light curve shows a steep decline, approximately simultaneously with the sharp optical decline. It reaches a minimum about 2 days later. The UV data after the day $T_0 + 27.5$ have been excluded due to contamination.

The X-ray observations (0.3–10.0 keV) start 1 day after the rise in the optical, approximately at the time of the optical peak. Our data do not cover the rise of the X-rays, thus we are not able to quantify any delay between the optical and X-ray rise, such as that observed, for example, by Wheatley, Mauche & Mattei (2003) in SS Cyg. In GW Lib, the X-ray flux is initially approximately three orders of magnitude above its pre-outburst quiescent level (Hilton et al. 2007), and it declines rapidly for ∼10 days before continuing to decline more slowly during the remainder of the optical outburst. Around day $T_0 + 26$, the flux dips sharply from log $F \approx -11.6$ erg cm^{-2} s^{-1} to log $F \approx -12.0$ erg cm^{-2} s^{-1}, lasting for less than a day. We have checked these data carefully and it is clear that this is a real dip in

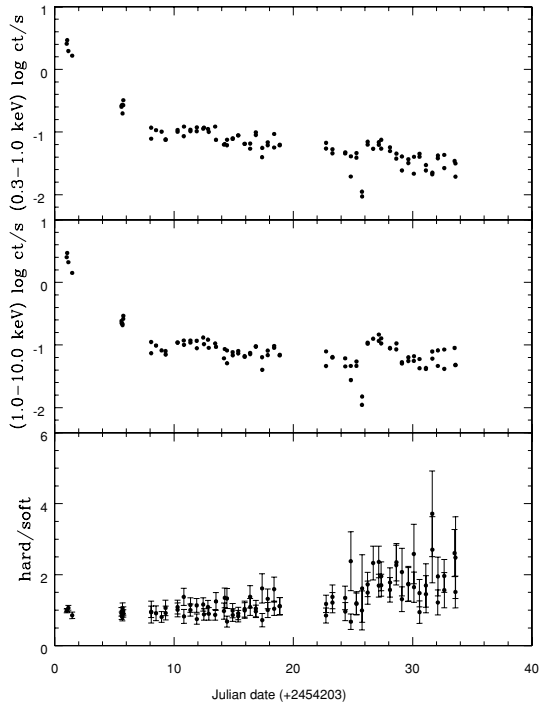

Figure 2. The soft (0.3–1.0 keV; upper panel) light curve, the hard (1.0–10.0 keV; middle panel) light curve and the X-ray hardness ratio (hard/soft) of GW Lib. The data have been binned at 700 s.

the brightness of the source. After the dip, the X-rays rise to the level of log $F \approx -11.2$ erg cm^{-2} s^{-1} and show a bump between days $T_0 + 26$ and $T_0 + 29$, which peaks at approximately the same time that the UV light curve finishes its steep decline. From $T_0 +$ 29 days onwards, the X-ray flux remains approximately constant at ~ -11.5 erg cm^{-2} s^{-1}.

During the two follow-up *Swift* observations in 2008, the count rate was consistent on days $T_0 + 378$ and $T_0 + 392$ at 0.03 ± 0.01 cts s^{-1}. In 2009, 682 and 690 days since T_0, it was 0.04 ± 0.01 cts s^{-1}. For comparison, Hilton et al. (2007) report a quiescence count rate of 0.02 cts s^{-1} (0.2–10.0 keV) in the *XMM–Newton* pn camera on 2005 August 25 and 26, about 2 years before the outburst. Assuming a thermal bremsstrahlung model of $kT = 3$ keV, this corresponds to an XRT count rate of 0.002 cts s^{-1}, where we used WEBPIMMS[2] to make the conversion. Thus, the X-ray flux seems to have remained an order of magnitude above the pre-outburst quiescent level for about 2 years after the outburst.

Fig. 2 shows the soft X-ray light curve (upper panel) in the 0.3–1.0 keV band and the hard X-ray light curve (middle panel) in the 1.0–10.0 keV band from the outburst observations. The lower panel shows the hardness ratio (extracted by using the tools of Evans et al. 2009). The hardness ratio gradually increases during the outburst, and shows a sharp increase at the time of the bump in the X-ray light curve, which coincides with the steep decline in the optical and UV light curves.

3.2 Search for oscillations in the X-ray data

Pulsations were discovered in the quiescent optical emission of GW Lib by Warner & van Zyl (1998). Pulsation periods near 230, 370 and 650 s are seen in the optical and UV wavebands (e.g. van Zyl

[2] http://heasarc.gsfc.nasa.gov/Tools/w3pimms.html

et al. 2004; Szkody et al. 2002) and an optical 2.1 h modulation was discovered by Woudt & Warner (2002). Copperwheat et al. (2009) found that the pulsation periods were suppressed after the 2007 outburst, but that the 2.1 h modulation remained.

Hilton et al. (2007) searched for these modulations in the *XMM–Newton* X-ray data taken during quiescence before the outburst, but did not detect any significant periodicities. They measured an upper limit of 0.092 mag for the X-ray pulsations.

We searched for periodicities from the outburst data by using two methods. When examining shorter time-scales, we took power spectra of near continuous sections of data, applying the normalization of Leahy et al. (1983) which allows the noise powers to be easily characterized so that detection limits can be set (see also Lewin, Paradijs & van der Klis 1988). For this method, the WT mode data were binned into 1 s time bins and the PC mode data into 5 s bins, which gave approximately 512 and 256 time bins per Fourier transform from individual *Swift* orbits, respectively. This gave 13 transforms for the WT mode and 48 for the PC mode, from which the averaged power spectrum was constructed for each mode. At the 99 per cent confidence level, no periodicities were seen in the data with a fractional amplitude upper limit of 6 per cent (WT mode) over the period range 2–512 s and 11 per cent (PC mode) over the period range 10–640 s.

When searching for longer time-scale modulations, notably at 650 s and 2.1 h (∼7560 s), as seen previously by the authors mentioned above, we initially calculated Lomb–Scargle periodograms of the data. Unfortunately, the identification of any potentially real modulation in the WT mode data at these time-scales was hindered by the window function caused by the light-curve sampling. However, by folding the PC mode data at the previously seen longer periods and at the orbital period ($P_{\rm orb}$ = 76.78 min; Thorstensen et al. 2002) we estimated 99 per cent upper limits to the fractional amplitude of any modulation at 650 s, 76.78 min (∼4607 s) and 7560 s to be 7, 6 and 8 per cent, respectively.

4 SPECTRAL ANALYSIS

4.1 Outburst X-ray spectra

Five X-ray spectra were extracted from the outburst observations to investigate the spectral evolution. The first and the second spectra, S1 and S2, consist of single observations (WT mode data) covering days T_0 + 1–2 and 6, respectively. The last three spectra, S3, S4 and S5, were extracted by combining observations covering longer time intervals (PC mode data). These intervals are given in Table 2. The X-ray spectra were binned at 20 counts per bin using the FTOOL GRPPHA, and the spectral analysis was carried out using XSPEC11. Fig. 3 shows the X-ray spectra from the start of the outburst (top)

Table 2. The XRT spectra of GW Lib and the corresponding observations. The epoch is in days since T_0.

Spectrum	Epoch (d)
S1	1–2
S2	6
S3	8–19
S4	23–28
S5	28–34
S6	(2008 and 2009 data)

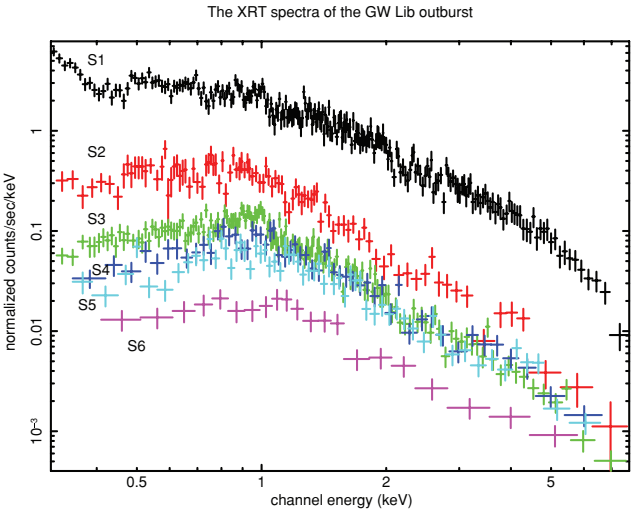

Figure 3. The X-ray spectra of GW Lib throughout the outburst.

until the end (bottom). The combined spectrum from the follow-up observations of 2008 and 2009 is also shown (labelled S6). The outburst spectra show that the increase in hardness apparent in Fig. 2 is due to a decrease in the relative strength of emission below about 1 keV. There is also excess soft X-ray emission apparent below 0.4 keV in the first observation (S1).

When DNe are in quiescence, the boundary layer is optically thin and assumed to be a source of hard X-rays (Pringle & Savonije 1979). During an outburst, the boundary layer is optically thick and emits more luminous soft X-ray emission which is usually described as blackbody emission (Pringle 1977). The optically thin hard X-ray component is usually somewhat suppressed in outburst.

The *Swift* XRT spectra shown in Fig. 3 are clearly dominated by hard X-ray emission, and so we started by fitting the first spectrum (S1) using an optically thin thermal plasma model (MEKAL model in XSPEC; Mewe, Lemen & van der Oord 1986; Liedahl, Osterheld & Goldstein 1995) with photoelectric absorption (WABS; Morrison & McCammon 1983) letting the abundance vary freely. This fit was not successful ($\chi^2_\nu/\nu = 3.35/226$), and a clear excess of soft photons was present below 0.7 keV. To account for this excess, we then added a blackbody component to the fit which improved ($\chi^2_\nu/\nu = 2.54/224$). There were still strong residuals between 0.5 and 0.7 keV suggesting that a second optically thin thermal emission model was needed. The abundances were still allowed to vary, but they were tied between the two optically thin emission models. With this model (a blackbody and two optically thin emission components with photoelectric absorption), we obtained a statistically acceptable fit to the S1 spectrum ($\chi^2_\nu/\nu = 1.11/222$). We tested whether a third optically thin emission component would improve the fit, and found a slightly better fit statistics of $\chi^2_\nu/\nu = 1.08/220$. Using the F-test, we found that this provides a better description of the underlying spectrum with a confidence of 98.5 per cent. Of course, these three distinct temperature components are most likely just an approximation to an underlying continuous distribution, such as the cooling flow models used by, for example, Wheatley et al. (1996b) and Mukai et al. (2003).

The data and the best-fitting model components for S1 with residuals are plotted in Fig. 4. The full set of fitted parameters is given in Table 3. It is worth noting that the fitted abundance is low, only $0.02^{+0.01}_{-0.01}$ times solar. We looked at this in some detail and found that the low abundance in our fit is driven entirely by the lack of thermal

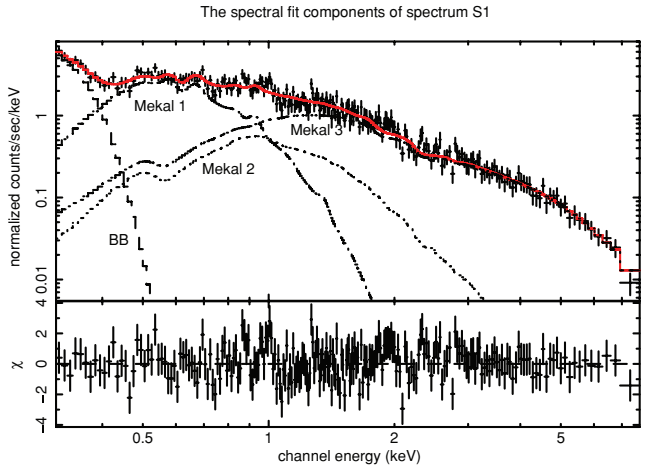

Figure 4. Upper panel: best-fitting model components of the first outburst spectrum (S1) of GW Lib. The data are fitted with a blackbody and three optically thin thermal emission components, all absorbed by the same column density. Lower panel shows the residuals.

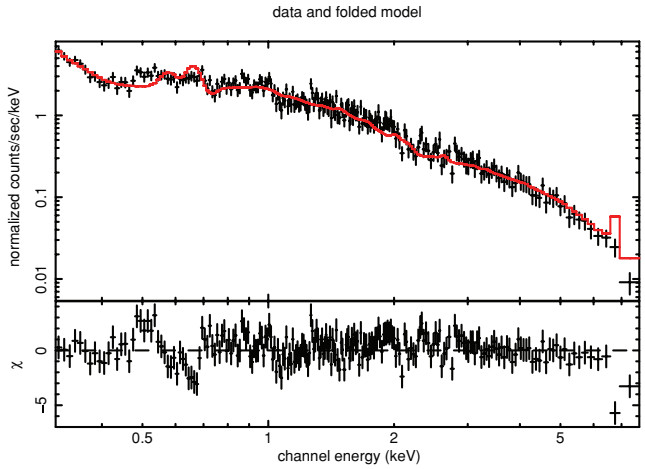

Figure 5. Upper panel: a spectral fit [a blackbody and three optically thin thermal emission models with variable abundances (VMEKAL)] to the first outburst spectrum (S1) with the oxygen abundance fixed to that found in the *XMM–Newton* quiescent spectrum by Hilton et al. (2007). An oxygen line of this strength (at 0.65 keV) would be detected and the fit is unacceptable with $\chi^2_\nu/\nu = 1.62/221$. The lower panel shows clear residuals between 0.55–0.70 and above 6.5 keV.

iron lines at around 6.7 keV. Strong line emission is predicted also by the model around 1 keV, but the spectral resolution here is not sufficient to provide strong constraints on abundances. Nevertheless, by fitting with a blackbody and three optically thin thermal emission models with variable abundances (VMEKAL), we found that the high oxygen abundance reported by Hilton et al. (2007) in GW Lib in quiescence (6–8 times solar) can be ruled out for our S1 spectrum. Setting the oxygen abundance to six times solar in our model resulted in an unacceptable best-fitting statistics of $\chi^2_\nu/\nu = 1.62/221$. This fit is plotted in Fig. 5.

In order to investigate the evolution of the X-ray spectra of GW Lib during the outburst, we tested the need for multitemperature optically thin emission components and for the blackbody in a similar manner for the second spectrum S2 and the subsequent spectra S3–S5. Since the abundances of the spectra S2–S5 were not well constrained, they were fixed to the best-fitting abundance of spectrum S1. There is no evidence for the presence of a blackbody

Table 3. The results of the spectral fitting using photoelectric absorption, blackbody and three optically thin emission components.

Spectrum model	S1 wa(bb+3me)	S2 wa(3me)	S3 wa(2me)	S4 wa(2me)	S5 wa(2me)
$n_{\rm H}$ (10^{20} cm^{-2})	$23.83^{+0.05}_{-0.04}$	$8.61^{+5.38}_{-3.99}$	$8.15^{+1.23}_{-1.17}$	$13.25^{+7.28}_{-3.38}$	$14.63^{+6.86}_{-4.36}$
$kT_{\rm bb}$ (keV)	$0.013^{+0.001}_{-0.001}$	–	–	–	–
kT_1 (keV)	$5.46^{+1.26}_{-0.86}$	$4.80^{+6.07}_{-1.66}$	$5.79^{+2.73}_{-1.51}$	$5.19^{+5.13}_{-1.88}$	$4.92^{+3.82}_{-1.36}$
kT_2 (keV)	$0.71^{+0.23}_{-0.13}$	$0.64^{+0.21}_{-0.14}$	$0.66^{+0.06}_{-0.07}$	$0.57^{+0.23}_{-0.24}$	$0.48^{+0.20}_{-0.16}$
kT_3 (keV)	$0.17^{+0.01}_{-0.01}$	$0.17^{+0.10}_{-0.05}$	–	–	–
F_1 (10^{-12} erg cm^{-2} s^{-1})	120.	6.72	3.05	3.88	3.62
F_2 (10^{-12} erg cm^{-2} s^{-1})	30.5	8.44	3.94	2.38	1.67
F_3 (10^{-12} erg cm^{-2} s^{-1})	271.	4.00	–	–	–
χ^2_ν/ν	1.08/220	1.25/89	1.13/150	0.94/50	1.19/56

Note. Not all components are fitted to all spectra. The errors correspond to the 90 per cent confidence limits for one parameter of interest. The measured abundance from the S1 spectrum is $0.02^{+0.01}_{-0.01}$, and the abundances in the other fits have been fixed at this value. The unabsorbed fluxes F_1, F_2 and F_3 correspond to the three optically thin emission components in the 0.3–10.0 keV band.

component in these spectra. Thus, a blackbody was not employed in the spectral fitting of the subsequent outburst spectra. The best fit for spectrum S2 was found with a photoelectric absorption and three optically thin emission components which yielded a goodness of fit of $\chi^2_\nu/\nu = 1.25/89$. The rest of the outburst spectra S3–S5 were fitted successfully with photoelectric absorption and two optically thin emission components. The best-fitting values, their 90 per cent confidence limits and the unabsorbed flux for each thermal emission component in the 0.3–10.0 keV range are given in Table 3. It can be seen that the increase in hardness towards the end of the outburst is due to a decrease in the relative quantity of cooler gas as the flux of the cooler temperature component drops in spectra S3–S5.

4.2 Fluxes, luminosities and accretion rates

The total fluxes, luminosities and accretion rates in the 0.3–10 keV range are given in Table 4. The fluxes given in the 0.3–10 keV range are absorbed fluxes. The distance was taken to be $r = 104$ pc (Thorstensen 2003). The accretion rates were estimated by using $\dot{M} = 2LR_{\rm WD}/GM_{\rm WD}$, where we adopt $M_{\rm WD} = 1\,{\rm M}_\odot$ and $R_{\rm WD} = 5.5 \times 10^8$ cm (Townsley, Arras & Bildsten 2004). The first X-ray spectrum gives a luminosity of 2.06×10^{32} erg s^{-1} which corresponds to $\dot{M} = 1.71 \times 10^{15}$ g s^{-1} or $2.7 \times 10^{-11}\,{\rm M}_\odot$ yr^{-1} in the 0.3–10 keV band. Since we do not see a rise in the X-rays, we are not able to say whether this is the peak luminosity of this outburst. We also derived the corresponding parameters for the bolometric luminosity by extrapolating our spectral fit over the range 0.0001–100 keV. The bolometric luminosity of the blackbody component in spectrum S1 is not well constrained, and the best-fitting value exceeds the Eddington limit of 1.3×10^{38} erg s^{-1} for the assumed mass; Fig. 6 shows the 68, 90 and 99 per cent confidence levels of $n_{\rm H}$ versus $kT_{\rm bb}$ and the corresponding range of bolometric luminosities. It can be seen that fits are allowed with much lower absorption column densities and luminosities. There is no reason to believe that the luminosity would exceed the Eddington limit. Estimating the luminosities of supersoft X-ray sources with blackbody models is notoriously unreliable (e.g. Krautter et al. 1996). Consequently, we do not attempt to give a bolometric luminosity for S1 in Table 4.

4.3 Later X-ray observations

We also determined the flux and luminosity for the individual integrated spectra of the 2008 and 2009 observations, and for the combined 2008+2009 spectrum. The spectra were fitted with an absorbed single-temperature optically thin thermal emission model. For the individual 2008 and 2009 spectra, we used Cash statistics due to the low number of counts. The spectral fitting parameters with fluxes and luminosities are given in Table 5. The abundance was

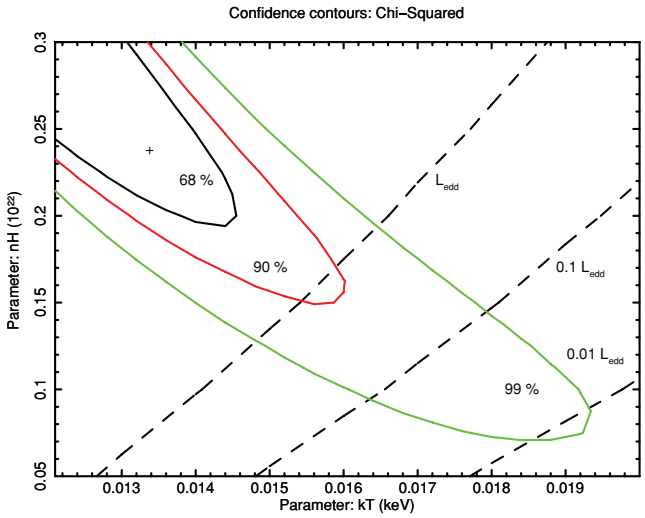

Figure 6. Blackbody parameters derived from the first outburst spectrum (S1) of GW Lib. The 10^{38} ($L_{\rm edd}$), 10^{37} (0.1 $L_{\rm edd}$) and 10^{36} erg s^{-1} (0.01 $L_{\rm edd}$) bolometric luminosity levels of the blackbody component are shown as dashed lines. The contours describe the 68, 90 and 99 per cent confidence levels for $n_{\rm H}$ versus $kT_{\rm bb}$.

unconstrained by the data and we fixed the value of $Z = 0.02\,{\rm Z}_\odot$ as obtained in outburst. The values in Table 5 show that the state of GW Lib did not change much between the 2008 and 2009 observations. Compared to the luminosity obtained by Hilton et al. (2007) before the outburst [$L(0.2\text{–}10\,{\rm keV}) = 9 \times 10^{28}$ erg s^{-1}], GW Lib is still an order of magnitude brighter in the *Swift* observations ∼2 years after the outburst.

4.4 Outburst UV spectra

Four background-subtracted source UV outburst spectra and one background spectrum are shown in Fig. 7. The observing dates corresponding to each spectrum are given in Table 6. They were chosen to represent the evolution of the UV data with time. The spectra show a blue continuum without strong emission or absorption lines, although weak features would be difficult to identify as the spectra suffer from modulo-8 fixed pattern noise. The top spectrum is an average of three source spectra corresponding to days $T_0 + 8$, 13 and 18 during the initial slow decline in Fig. 1. The two subsequent spectra are from days $T_0 + 23$ (before the steep decline) and $T_0 + 26$ (after the steep decline). The penultimate spectrum averages three spectra around day $T_0 + 27$, and the bottom spectrum shows the background flux for one of the source spectra on

Table 4. The fluxes, luminosities and accretion rates in the 0.3–10 keV (fluxes absorbed) and 0.0001–100 keV (bolometric, fluxes unabsorbed) bands of the XRT spectra.

Spectrum	Flux (erg cm^{-2} s^{-1}) (0.3–10 keV)	Luminosity (erg s^{-1}) (0.3–10 keV)	$\dot{M}$ (g s^{-1}) (0.3–10 keV)	Flux (erg cm^{-2} s^{-1}) (0.0001–100 keV)	Luminosity (erg s^{-1}) (0.0001–100 keV)	$\dot{M}$ (g s^{-1}) (0.0001–100 keV)
S1	1.60×10^{-10}	2.06×10^{32}	1.71×10^{15}	–	–	–
S2	1.25×10^{-11}	1.63×10^{31}	1.35×10^{14}	5.10×10^{-11}	6.66×10^{31}	5.52×10^{14}
S3	5.18×10^{-12}	6.66×10^{30}	5.52×10^{13}	1.12×10^{-11}	1.44×10^{31}	1.19×10^{14}
S4	4.38×10^{-12}	5.63×10^{30}	4.67×10^{13}	9.53×10^{-12}	1.23×10^{31}	1.02×10^{14}
S5	3.66×10^{-12}	4.71×10^{30}	3.89×10^{13}	8.12×10^{-12}	1.04×10^{31}	8.62×10^{13}

Table 5. The spectral fitting parameters with fluxes and luminosities of the 2008 and 2009 (Columns 2 and 3) X-ray observations of GW Lib. The fourth column shows the spectral fitting parameters for the combined 2008 and 2009 spectrum.

Parameter	2008	2009	2008+2009
$n_{\rm H}$ 10^{20} cm^{-2}	$7.23^{+5.74}_{-5.08}$	$5.63^{+5.09}_{-4.32}$	$0.11^{+4.45}_{-0.11}$
kT keV	$1.20^{+0.64}_{-0.33}$	$2.00^{+1.09}_{-0.64}$	$3.51^{+1.46}_{-1.16}$
F(0.3–10 keV) erg cm^{-2} s^{-1}	7.5×10^{-13}	8.5×10^{-13}	1.1×10^{-12}
L(0.3–10 keV) erg s^{-1}	9.8×10^{29}	1.1×10^{30}	1.4×10^{30}
$\dot{M}$(0.3–10 keV) g s^{-1}	8.2×10^{12}	9.1×10^{12}	1.2×10^{13}
F(0.0001–100 keV) erg cm^{-2} s^{-1}	1.4×10^{-12}	1.4×10^{-12}	1.3×10^{-12}
L(0.0001–100 keV) erg s^{-1}	1.8×10^{30}	1.8×10^{30}	1.7×10^{30}
$\dot{M}$(0.0001–100 keV) g s^{-1}	1.5×10^{13}	1.5×10^{13}	1.4×10^{13}

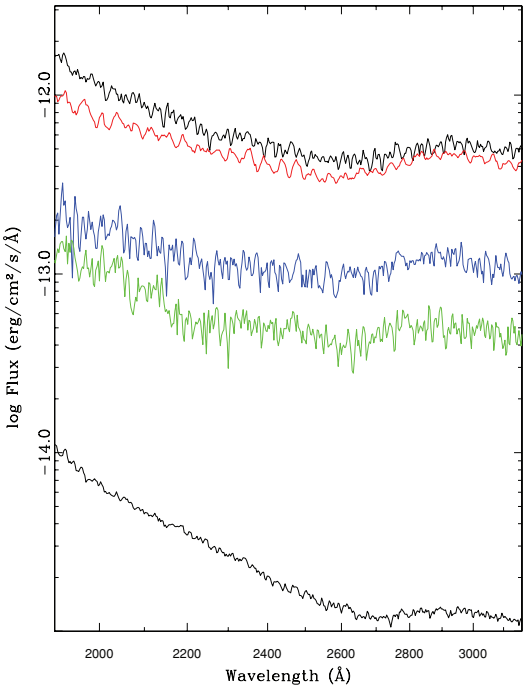

Figure 7. The evolution of the background-subtracted UVOT UV grism flux spectra of GW Lib throughout the outburst in descending and chronological order. The top spectrum is an average of three spectra corresponding to days $T_0 + 8$, 13 and 18. The following three spectra correspond to days $T_0 +$ 23, 26, and 27 (the spectrum on day $T_0 + 27$ is an average of three spectra during that day). The bottom spectrum shows the background flux level for one of the spectra on day $T_0 + 27$.

day $T_0 + 27$. It seems the spectra become less blue after the sharp decline. All of the spectra, including the background spectrum, show a bump around ∼2900 Å. This feature is most likely due to the contribution of the second-order spectrum (see 'Notes for observing with the UVOT UV grism[3]' which shows that for a calibration white dwarf the second-order UV light starts at ∼2800 Å). In the last two source spectra, the background noise features are becoming clearer when the source itself is becoming fainter.

The 2001 July *HST*/Space Telescope Imaging Spectrograph outburst spectrum of WZ Sge showed an Mg II absorption line at 2790–2810 Å (Kuulkers et al. 2002). Kuulkers et al. (2002) note that most of it originates from WZ Sge and part of it is due to interstellar absorption. This line is not seen in the UV spectra of GW Lib probably due to the much lower resolution of the UV grism.

The calibration of the UV grism is ongoing, and consequently absolute flux measurements remain uncertain. Nevertheless, we measured monochromatic fluxes at 2200 Å for the source spectra in Fig. 7 and obtained $\lambda F_{2200} \sim 1.49 \times 10^{-9}, 1.14 \times 10^{-9}, 2.13 \times 10^{-10}$, and 1.15×10^{-10} erg cm^{-2} s^{-1}, respectively. For $L = 4\pi r^2 F$ with $r = 104$ pc (Thorstensen 2003), the fluxes given above correspond to monochromatic luminosities $\lambda L_{2200} \sim 1.95 \times 10^{33}, 1.49 \times 10^{33}, 2.78 \times 10^{32}$ and 1.50×10^{32} erg s^{-1}.

Table 6. The observation dates since the onset of the outburst for the UV grism spectra in Fig. 7.

$T_0 +$	Obs date
8	2007-04-20
13	2007-04-25
18	2007-04-30
23	2007-05-05
26	2007-05-08
27	2007-05-09

Table 7. The average magnitudes, fluxes and their 1σ errors in the UVOT V and $UVW1$ ($\bar{\lambda} = 2600$ Å) filters for the 2008 and 2009 observations of GW Lib. The magnitudes and fluxes are the mean values of different snapshots. Observation time corresponds to the midpoint of each observation in days since T_0. The exposure times are given in Table 1.

Obs ID	Obs time (d)	Filter	Magnitude (mag)	log flux (erg s^{-1} cm^{-2} Å^{-1})
7042	378.25	V	16.37 ± 0.01	-14.979 ± 0.005
7042	378.25	$UVW1$	14.69 ± 0.01	-14.277 ± 0.002
7043	385.21	V	16.40 ± 0.07	-14.987 ± 0.030
7044	392.04	V	16.39 ± 0.02	-14.987 ± 0.009
7044	392.04	$UVW1$	14.60 ± 0.01	-14.243 ± 0.004
7045	682.08	V	16.54 ± 0.01	-15.042 ± 0.005
7045	682.08	$UVW1$	14.84 ± 0.01	-14.339 ± 0.002
7046	689.81	V	16.53 ± 0.02	-15.039 ± 0.006
7046	689.81	$UVW1$	14.84 ± 0.01	-14.338 ± 0.003

4.5 Later UV observations

We studied the follow-up UVOT observations from 2008 and 2009 in order to see how the UV magnitudes and fluxes have changed since the outburst. The results are given in Table 7. Since the last measurement in the outburst light curve, the UV flux has faded by 0.8 in log F.

[3] http://swift.gsfc.nasa.gov/docs/swift/analysis/uvot_ugrism.html

5 DISCUSSION

In most cases, the hard X-ray emission of DNe is suppressed during an outburst. This is the case for VW Hyi (Wheatley et al. 1996b), SS Cyg (Ricketts, King & Raine 1979; Jones & Watson 1992; Wheatley et al. 2003), Z Cam (Wheatley et al. 1996a), YZ Cnc (Verbunt, Wheatley & Mattei 1999) and WZ Sge (Wheatley & Mauche 2005). In contrast, the outburst X-ray emission of GW Lib peaks at two to three orders of magnitude higher than its quiescent level obtained by *XMM–Newton* in 2005 (Hilton et al. 2007). U Gem is the only other DN seen to increase its X-ray luminosity during an outburst (Swank et al. 1978), and in this case the outburst emission is only about a factor of 5 above its quiescent level (Mattei, Mauche & Wheatley 2000).

The absolute luminosity of the peak X-ray emission of GW Lib is high, but not extraordinary (Table 4). It is about a factor of 2 less than the X-ray luminosity of SS Cyg at optical maximum (which corresponds to the second, weaker peak in the X-ray light curve of SS Cyg; Wheatley et al. 2003), and it is only a factor of 2 more luminous than RU Peg in outburst and a factor of 3 brighter than SU UMa in outburst (Baskill, Wheatley & Osborne 2005). GW Lib seems to stand out due to its unusually low X-ray luminosity in quiescence, rather than an exceptional X-ray luminosity in outburst. It may be that the relatively high mass of the white dwarf (Townsley et al. 2004) accounts for the high outburst X-ray luminosity, as it may do also in SS Cyg.

Very few systems have good X-ray coverage during an outburst, so it is not clear whether the steep decline in the X-ray luminosity of GW Lib during the first 10 days of outburst is typical of other systems. The X-ray flux of WZ Sge itself does decline during the first half of the outburst (Wheatley & Mauche 2005), but only about a factor of 3 in 10 days, compared with a factor of 30 in GW Lib also over 10 days (although note that the first X-ray observation of WZ Sge occurred about 3 days after the optical maximum). SS Cyg also declined after the optical maximum, in this case by about a factor of 6 over 7 days (Wheatley et al. 2003). In contrast, the X-ray flux of VW Hyi was approximately constant during the outburst (Wheatley et al. 1996b).

In most DNe, the dominant high-energy emission during an outburst is optically thick emission from the boundary layer, which emerges in the extreme-UV (Pringle 1977). This seems also to be the case for GW Lib, with a supersoft component detected in the first *Swift* observation, although the luminosity of this component is poorly constrained by our observations (Fig. 6). The supersoft component is detected only in our first observation, but it is likely to be present also in the later epochs and just too soft to be detected by the *Swift* XRT. Only a small spectral change would be needed to move this component out of our bandpass. Indeed, the extreme-UV components of VW Hyi and WZ Sge are not detected at all with the *ROSAT* Position Sensitive Proportional Counter (PSPC) and the *Chandra* AXAF CCD Imaging Spectrometer X-ray detectors, respectively (Wheatley et al. 1996b; Wheatley & Mauche 2005), although they are detected in the *EXOSAT* low energy telescope and *Chandra* low-energy transmission grating bandpasses.

In the few cases where good coverage has been achieved, the extreme-UV emission rises only after the X-ray emission has been suppressed (e.g. Jones & Watson 1992; Wheatley et al. 1996a, 2003), and it is assumed that this supersoft component takes over as the main source of cooling as the boundary layer becomes optically thick to its own emission. Since the extreme-UV emission is present even in our first *Swift* observation, it is possible that the observed peak in X-ray emission actually represents the suppressed level, and that an even stronger X-ray peak was missed, corresponding to the peak emission of the optically thin boundary layer. In SS Cyg, this first X-ray peak is a factor of 3 brighter than the second, weaker peak corresponding to the optical maximum.

In our later *Swift* observations, the X-rays decline, then flatten off, and at the end of the disc outburst there is a sharp dip followed by a bump in the X-ray light curve, which coincides with the rapid decline in the optical and UV light curves. The X-ray hardness also increases at this time. These features are shared to some extent with other systems. A dip and a bump are seen in U Gem (Mattei et al. 2000) which is the only other system where X-rays are known to be brighter in outburst than in quiescence. A bump is also seen in SS Cyg where it is thought to correspond to the boundary layer transitioning back to its optically thin state (Wheatley et al. 2003). Another feature similar to GW Lib is the increase in hardness at the end of the outburst in SS Cyg, and indeed DNe are usually harder in quiescence than in outburst (Baskill et al. 2005).

When comparing the outburst X-ray emission to quiescence, it is important to distinguish between pre- and post-outburst quiescence. GW Lib was unusually faint for a DN in quiescence in the *XMM–Newton* observation made 2 years before the 2007 outburst (Hilton et al. 2007). Our *Swift* XRT outburst observations continued for about 6 days after the end of the sharp decline in the optical and UV light curves, which presumably defines the end of the disc outburst. Our measured X-ray luminosity after this decline (S5 in Table 4) is a factor of 50 higher than the pre-outburst quiescent level (Hilton et al. 2007). Our follow-up *Swift* observations in 2008 and 2009 show that GW Lib declined by a factor of 5 after the outburst, but it remained an order of magnitude brighter than the pre-outburst observations for at least 21 months after the outburst. Another important difference between the *XMM–Newton* and *Swift* observations is that Hilton et al. (2007) found an oxygen abundance enhanced by at least a factor of 6 above the solar value, whereas we find that our first outburst spectrum is inconsistent with such a high value and that the iron abundance appears to be significantly subsolar. It is difficult to understand how observed abundances can change so much between quiescence and outburst.

It has been noted in other systems that the X-ray flux tends to decrease between outbursts. Examples include VW Hyi (van der Woerd & Heise 1987) and SS Cyg (McGowan, Priedhorsky & Trudolyubov 2004). This is in contrast to the usual predictions of the disc instability model (e.g. Lasota 2001) in which the accretion rate gradually increases during quiescence as the disc refills. The inferred decrease in the quiescent X-ray flux in GW Lib is by a much larger factor than in VW Hyi and SS Cyg, but the interoutburst interval is also much larger in GW Lib (decades compared with weeks and months), so there is more time for this decrease to progress.

5.1 Possible disc models

The long interoutburst intervals of GW Lib and other WZ Sge type stars mean that the opportunities to study the outbursts of these objects in detail have been very scarce. In this respect, our data represent a rare insight into these intriguing DNe.

To date, the physical cause of the long interoutburst times has remained elusive. It is not at all clear why the accretion discs in these stars should behave any differently from those in other DNe with very similar system parameters. Yet, while the majority of non-magnetic, short-period DNe exhibit outbursts every few weeks or months, the WZ Sge stars outburst every few years or decades. There are two main sets of models which attempt to explain this

stark difference in recurrence time. In order to suppress the onset of regular outbursts and hence lengthen the interoutburst interval, either the quiescent viscosity must be much lower than in other systems (Smak 1993; Howell, Szkody & Cannizzo 1995) or the inner disc must be somehow truncated (Warner, Livio & Tout 1996; Matthews et al. 2007). While the low-viscosity models are appealing in that they neatly explain the long recurrence times, they remain unsatisfying in requiring the viscosity in some quiescent discs to be different from others while, at the same time, being very similar during outbursts. Models which appeal to inner-disc truncation suppress regular outbursts by removing the inner region of the accretion disc where outbursts are most easily triggered. Often disc truncation is explained by the propeller action of the torque exerted on the accretion disc caused by a magnetic field anchored on a rapidly rotating primary star (Warner et al. 1996; Matthews et al. 2007) (a white dwarf magnetic field strength of $B \sim 10^5$ G was assumed for WZ Sge by Matthews et al. 2007). In this case, mass would accumulate at large radii leaving a truncated and stabilized (with respect to frequent DNe outbursts) outer disc which acts as a large reservoir of mass. If the same physical mechanism was responsible for the long interoutburst time-scales of all of the WZ Sge stars, it may be reasonable to expect their outbursts to look very similar. In this respect, the differences between the observed outburst properties of GW Lib and WZ Sge, as outlined above, are puzzling.

The detailed emission physics of the magnetic propeller models in particular is not well understood, making theoretical predictions of multiwavelength outburst light curves extremely difficult. However, we note that both the low-viscosity and disc truncation mechanisms tend to reduce the accretion rate during quiescence and may explain the low and decreasing X-ray flux in GW Lib between outbursts. Also, in the case of GW Lib, the X-rays are quenched on a time-scale of $\sim$10 days. The only plausible time-scale close to this value is the viscous time of the accretion disc. Interpreting this as a viscous time-scale, $t_{\rm visc} \sim R^2/\alpha_{\rm H} c_{\rm s} H$, we obtain an associated radius of $R \sim 10^{10}$ cm, where we have assumed that the viscosity in the hot state $\alpha_{\rm H} = 0.1$, sound speed $c_{\rm s} = 10$ km s^{-1} and disc scaleheight = 0.1 R. This estimate is interesting as it is close to the required values for disc truncation. Thus, it is conceivable that the quenching of the X-ray flux is associated with the inward progression of the accretion disc towards the white dwarf, and the eventual development of a boundary layer, once the outburst has been triggered.

6 CONCLUSIONS

We have obtained optical, UV and X-ray observations of the 2007 outburst of the WZ Sge type DN GW Lib. GW Lib stands out as the second known DN, in addition to U Gem, where hard X-rays are not suppressed during outburst. Rather than having a remarkably high X-ray luminosity in an outburst, GW Lib has a very low X-ray luminosity in quiescence compared to other DNe. The outburst X-ray light curve of GW Lib shows some similarities with other DNe, such as a bump seen at the end of the X-ray light curve and hardening of the X-rays towards the end of the outburst. These features are also seen in SS Cyg. WZ Sge and GW Lib show some differences in their outburst data: the hard X-rays in WZ Sge are suppressed and the X-rays decline with a much smaller factor in the beginning of the X-ray light curve compared to GW Lib.

A supersoft component, which probably originates from the optically thick boundary layer, is detected in the first outburst spectrum. Other systems, such as VW Hyi and WZ Sge, also show this component in their outburst data. The spectral resolution of the *Swift* XRT or UVOT is not sufficient to distinguish emission or absorption lines in the spectra.

The outburst X-ray luminosity at the optical maximum was three orders of magnitude higher than during the pre-outburst quiescence level in 2005. GW Lib was still an order of a magnitude brighter during the 2008 and 2009 post-outburst observations than during the pre-outburst observations.

The long recurrence time and the lack of normal outbursts suggest that the structure of the accretion disc could be explained by models which favour very long recurrence times. The two main categories for these models are (1) low disc viscosity in quiescence and (2) a truncated inner disc due to a magnetic propeller white dwarf. Assuming that the outbursts of all WZ Sge stars would be driven by a similar physical mechanism, the observed differences in the outburst data of GW Lib and WZ Sge are perplexing.

ACKNOWLEDGMENTS

KB acknowledges funding from the European Commission under the Marie Curie Host Fellowship for Early Stage Research Training SPARTAN, Contract No MEST–CT–2004–007512, University of Leicester, UK. The authors also acknowledge the support of STFC. We acknowledge with thanks the variable star observations from the AAVSO International Data base contributed by observers worldwide and used in this research. We thank the *Swift* science team and planners for their support of these target-of-opportunity observations. *Swift* data were extracted from the *Swift* science archive at www.swift.le.ac.uk. This work made use of data supplied by the UK *Swift* Science Data Centre at the University of Leicester. The WASP Consortium consists of astronomers primarily from Queen's University Belfast, Keele, Leicester, The Open University, and St Andrews, the Isaac Newton Group (La Palma), the Instituto de Astrofísica de Canarias (Tenerife) and the South African Astronomical Observatory. The SuperWASP-N and WASP-S Cameras were constructed and operated with funds made available from Consortium Universities and the UK's Science and Technology Facilities Council. WASP-South is hosted by the South African Astronomical Observatory (SAAO), and we are grateful for their support and assistance. We thank M. R. Goad for helpful comments on this paper.

REFERENCES

Baskill D. S., Wheatley P. J., Osborne J. P., 2005, MNRAS, 357, 626
Burrows D. N. et al., 2005, Space Sci. Rev., 120, 165
Capalbi M., Perri M., Saija B., Tamburelli F., Angelini L., 2005, The Swift XRT Data Reduction Guide, Version 1.2 (http://heasarc.nasa.gov/docs/swift/analysis/xrt_swguide_v1_2.pdf)
Copperwheat C. M. et al., 2009, MNRAS, 393, 157
Evans P. A. et al., 2009, MNRAS, 397, 1177
Duerbeck H. W., Seitter W. C., 1987, Ap&SS, 131, 467
Gehrels N. et al., 2004, ApJ, 611, 1005
Hassall B. J. M., Pringle J. E., Schwarzenberg-Czerny A., Wade R. A., Whelan J. A. J., Hill P. W., 1983, MNRAS, 203, 865
Hilton E. J., Szkody P., Mukadam A., Mukai K., Hellier C., van Zyl L., Homer L., 2007, AJ, 134, 1503
Hoshi R., Prog. Theor. Phys., 1979, 61, 1307
Howell S. B., Szkody P., Cannizzo J. K., 1995, ApJ, 439, 337
Immler S. et al., 2006, The SWIFT UVOT Software Guide, Version 2.0, NASA/GSFC
Jones M. H., Watson M. G., 1992, MNRAS, 257, 633
Koester D., Chanmugam G., 1990, Rep. Prog. Phys., 53, 837
Krautter J., Ögelman H., Starrfield S., Wichmann R., Pfeffermann E., 1996, ApJ, 456, 788

Kuulkers E., Knigge C., Steeghs D., Wheatley P. J., Long K. S., 2002, in Gänsicke B. T., Beuermann K., Reinsch K., eds, ASP Conf. Ser. Vol. 261, The Physics of Cataclysmic Variables and Related Objects. Astron. Soc. Pac., San Francisco, p. 443
Lasota J.-P., 2001, New Astron. Rev., 45, 449
Leahy D. A., Darbro W., Elsner R. F., Weisskopf M. C., Kahn S., Sutherland P. G., 1983, ApJ, 266, 160
Lewin W. H. G., van Paradijs J., van der Klis M., 1988, Space Sci. Rev., 46, 273
Liedahl D. A., Osterheld A. L., Goldstein W. H., 1995, ApJ, 438, L115
McGowan K. E., Priedhorsky W. C., Trudolyubov S. P., 2004, ApJ, 601, 1100
Mattei J. A., Mauche C., Wheatley P. J., 2000, JAVSO, 28, 160
Matthews O. M., Speith R., Wynn G. A., West R. G., 2007, MNRAS, 375, 105
Mauche C. W., Raymond J. C., 2000, ApJ, 541, 924
Maza J., Gonzalez L. E., 1983, IAU Circ., 3854, 2
Mewe R., Lemen J. R., van den Oord G. H. J., 1986, A&AS, 65, 511
Morrison R., McCammon D., 1983, ApJ, 270, 119
Mukai K., Kinkhabwala A., Peterson J. R., Kahn S. M., Paerels F., 2003, ApJ, 586, L77
Pollacco D. et al., 2006, PASP, 118, 1407
Pringle J. E., 1977, MNRAS, 178, 195
Pringle J. E., Savonije G. J., 1979, MNRAS, 187, 777
Pringle J. E. et al., 1987, MNRAS, 225, 73
Ricketts M. J., King A. R., Raine D. J., 1979, MNRAS, 186, 233
Romano P. et al., 2006, A&A, 456, 917
Roming P. W. A. et al., 2005, Space Sci. Rev., 120, 95
Smak J., 1993, Acta Astron., 43, 101
Swank J. H., Boldt E. A., Holt S. S., Rothschild R. E., Serlemitsos P. J., 1978, ApJ, 226, L133
Szkody P., Gänsicke B. T., Howell S. B., Sion E. M., 2002, ApJ, 575, 79
Templeton M. R., 2007, AAN, 349, 1
Thorstensen J. R., Patterson J., Kemp J., Vennes S., 2002, PASP, 114, 1108
Thorstensen J. R., 2003, AJ, 126, 3017
Townsley D. M., Arras P., Bildsten L., 2004, ApJ, 608, L105
van der Woerd H., Heise J., 1987, MNRAS, 225, 141
van Zyl L., Warner B., O'Donoghue D., Sullivan D., Pritchard J., Kemp J., 2000, Balt. Astron., 9, 231
van Zyl L. et al., 2004, MNRAS, 350, 307
Verbunt F., Wheatley P. J., Mattei J. A., 1999, A&A, 346, 146
Warner B., van Zyl L., 1998, in Deubner F.-L., Christensen-Dalsgaard J., Kurtz D., eds, Proc. IAU Symp. 185, New Eyes to See Inside the Sun and Stars. Kluwer, Dordrecht, p. 321
Warner B., Livio M., Tout C. A., 1996, MNRAS, 282, 735
Wheatley P. J., Mauche C. W., 2005, in Hameury J. M., Lasota J. P., eds, ASP Conf. Ser. Vol. 330, The Astrophysics of Cataclysmic Variables and Related Objects. Astron. Soc. Pac., San Francisco, p. 257
Wheatley P. J., van Teeseling A., Watson M. G., Verbunt F., Pfeffermann E., 1996a, MNRAS, 283, 101
Wheatley P. J., Verbunt F., Belloni T., Watson M. G., Naylor T., Ishida M., Duck S. R., Pfeffermann E., 1996b, A&A, 307, 137
Wheatley P. J., Mauche C. W., Mattei J. A., 2003, MNRAS, 345, 49
Whitehurst R., 1988, MNRAS, 232, 35
Woudt P. A., Warner B., 2002, Ap&SS, 282, 433

This paper has been typeset from a TEX/LATEX file prepared by the author.